

of the background. Motion-defined figures could (randomly) appear at one of three possible locations (eccentricity: 2.7° to 4.4°).

2. Multiunit activity was recorded through 16 micro-wire electrodes in each monkey (4, 6). Receptive-field size ranged from 0.7° to 1.4° (median 0.9°), and eccentricity from 1.3° to 2.8° in one monkey and from 3.4° to 5.7° in the other. For each monkey, figure positions and electrodes were chosen such that the figures covered the receptive fields of 16 electrodes simultaneously.

3. Data were obtained in pseudo-randomly interleaved blocks of trials in 9 to 12 daily sessions. To ensure identical receptive-field stimulation for figure and background responses, we compared the responses to the same directions of motion for figure and ground and averaged the responses to the different directions of motion. Electrophysiological data obtained during the interval between stimulus onset and cue time were analyzed. Response strength was calculated as the average normalized activity during the intervals. Contextual modulation was calculated by subtracting the background response strength from

the figure response strength. For all statistics, paired *t* tests were applied.

4. V. A. F. Lamme, K. Zipser, H. Spekreijse, *Proc. Natl. Acad. Sci. U.S.A.* **95**, 3263 (1998).

5. V. A. F. Lamme, H. Supèr, R. Landman, P. R. Roelfsema, H. Spekreijse, *Vision Res.* **40**, 1507 (2000).

6. H. Supèr, H. Spekreijse, V. A. F. Lamme, *Nature Neurosci.* **4**, 304 (2001).

7. J. M. Hupé *et al.*, *Nature* **394**, 784 (1998).

8. V. A. F. Lamme, H. Supèr, H. Spekreijse, *Curr. Opin. Neurobiol.* **8**, 529 (1998).

9. B. R. Payne, S. G. Lomber, A. E. Villa, J. Bullier, *Trends. Neurosci.* **19**, 535 (1996).

10. For the static figure-ground texture, we used line segments that were 16 by 1 pixels (0.44° by 0.027°) and the density was five line segments per square degree. Two different line segment orientations (135° or 45°) were used to segregate figure from ground, and both line orientations were used for figure and background.

11. J. M. Fuster, *Trends. Neurosci.* **20**, 451 (1997).

12. The motion defined figure-ground display was identical to that described before, except that during the

delay period a second stimulus (red circle: size 2° to 3°, eccentricity: 5.5° to 6°) appeared in one of three positions but different from that of the figure location. For this task, another monkey was also used. Data were obtained in blocked 10 to 12 daily sessions and normalized as described in (3).

13. Y. Miyashita, H. S. Chang, *Nature*, **331**, 68 (1988).

14. P. S. Goldman-Rakic, in *Progress in Brain Research*, H. B. M. Uylings, C. G. P. van Eden, J. P. C. D. de Bruin, M. A. Corner, M. G. P. Feenstra, Eds. (Elsevier, Amsterdam, 1990), pp. 313–323.

15. S. M. Courtney, L. G. Ungerleider, K. Keil, J. V. Haxby, *Nature* **386**, 608 (1997).

16. V. Di Lollo, *J. Exp. Psychol. Hum. Percept. Perform.* **10**, 144 (1984).

17. S. Shiori, P. Cavanagh, *Vision Res.* **32**, 943 (1992).

18. We thank K. Brandsma and J. de Feiter for biotechnical support, and P. Brassinga and H. Meester for technical assistance. H.S. is supported by a grant of Medical Science (MW) from Netherlands Organization for Scientific Research (NWO).

7 March 2001; accepted 23 May 2001

Stimulation of RNA Polymerase II Elongation by Hepatitis Delta Antigen

Yuki Yamaguchi,¹ Julija Filipovska,² Keiichi Yano,³ Akiko Furuya,³ Naoto Inukai,¹ Takashi Narita,¹ Tadashi Wada,¹ Seiji Sugimoto,³ Maria M. Konarska,² Hiroshi Handa^{1*}

Transcription elongation by RNA polymerase II (RNAPII) is negatively regulated by the human factors DRB-sensitivity inducing factor (DSIF) and negative elongation factor (NELF). A 66-kilodalton subunit of NELF (NELF-A) shows limited sequence similarity to hepatitis delta antigen (HDAG), the viral protein required for replication of hepatitis delta virus (HDV). The host RNAPII has been implicated in HDV replication, but the detailed mechanism and the role of HDAG in this process are not understood. We show that HDAG binds RNAPII directly and stimulates transcription by displacing NELF and promoting RNAPII elongation. These results suggest that HDAG may regulate RNAPII elongation during both cellular messenger RNA synthesis and HDV RNA replication.

The human transcription elongation factors DSIF and NELF bind RNAPII and repress the elongation activity of this polymerase (1–4). This repression is reversed by P-TEFb, a positive elongation factor with a protein kinase activity that phosphorylates the COOH-terminal domain (CTD) of RNAPII and a subunit of DSIF (5), in a manner sensitive to the kinase inhibitors 5,6-dichloro-1-beta-D-ribofuranosylbenzimidazole (DRB) and H8. Because DRB affects the synthesis of most mRNAs, the DRB-sensitive elongation involving DSIF, NELF, and P-TEFb may reflect a general rate-limiting step of RNAPII transcription (6). The yeast homologs of

DSIF, transcription factors Spt5 and Spt4, have been shown to affect elongation (7). Purified NELF is composed of five polypeptides, A to E, the smallest of which, NELF-E (46 kD), is identical to a putative RNA-binding protein (4). We microsequenced NELF-A (66 kD) and found it to be encoded by *WHSC2* (Fig. 1A), a candidate gene for the Wolf-Hirschhorn syndrome, a multiple malformation syndrome characterized by mental and developmental defects resulting from a deletion in chromosome 4p16.3 (8). Computer analyses identified a weak sequence similarity (27% identity) between the NH₂-terminal half of NELF-A/*WHSC2* (amino acids 89 to 248) and HDAG, the sole protein encoded by HDV, with the similarity extending to the predicted secondary structures of these proteins (Fig. 1B).

HDV, a satellite of hepatitis B virus, has a ~1700-nucleotide (nt) circular, single-stranded RNA genome with a rodlike structure (9). Replication of HDV RNA appears to involve the

host RNAPII and requires the presence of HDAG (9–11). Two forms of HDAG, HDAG-S (195 amino acids long) and HDAG-L (214 amino acids long), originate from editing of the common mRNA. Both forms bind HDV RNA, but have distinct roles in the viral life cycle. HDAG-S activates HDV replication, whereas HDAG-L, which contains a 19-amino acid COOH-terminal extension, inhibits replication and directs virion assembly (9–12). Earlier reports have implicated HDAGs in both activation and inhibition of RNAPII transcription (13, 14), but the nature of this discrepancy and the mechanism of HDAG action are unknown.

To investigate if, and how, HDAGs regulate RNAPII transcription, we examined the effect of HDAG on DNA-templated transcription using HeLa nuclear extracts (NE). In the presence of DRB, endogenous DSIF/NELF can repress transcription (Fig. 2A) (4). HDAGs reversed this inhibition (HDAG-S was more effective than HDAG-L), with little effect on basal (–DRB) transcription (Fig. 2A). This effect required NELF, because NE immunodepleted of NELF failed to respond to HDAGs (Fig. 2B). These results suggest that HDAG stimulates RNAPII transcription by counteracting the negative effect of DSIF/NELF.

Because HDAG does not affect the kinase activity of P-TEFb or CTD phosphorylation (15), we sought to determine whether it affects association of NELF, DSIF, and RNAPII under transcription conditions. In NE prepared from HeLa cells expressing Flag-NELF-E, antibodies to Flag (anti-Flag) immunoprecipitated the other NELF subunits (15), DSIF, and RNAPII (Fig. 3A) (4). Preincubation of the NE with HDAG-S substantially reduced the levels of DSIF and RNAPII in the precipitate (Fig. 3A), but had little effect on DSIF-RNAPII interaction (15). To determine the direct target of HDAG, we analyzed the NE proteins associated with glutathione *S*-transferase (GST)–HDAG. Under

¹Frontier Collaborative Research Center, Tokyo Institute of Technology, 4259 Nagatsuta, Yokohama 226–8503, Japan. ²Rockefeller University, New York, NY 10021, USA. ³Tokyo Research Laboratories, Kyowa Hakko Kogyo, Machida, Tokyo 194–8533, Japan.

*To whom correspondence should be addressed. E-mail: hhanda@bio.titech.ac.jp

REPORTS

saturating concentrations, both GST-HDAg-L and GST-HDAg-S, but not GST alone, bound to substantial amounts of RNAPII (Fig. 3B). In addition, small amounts of DSIF, but not NELF, were found associated with GST-HDAg (Fig. 3B). These results suggest that HDAg directly binds RNAPII and inhibits NELF-RNAPII association, possibly because HDAg competes with NELF-A for a common surface on RNAPII, without substantially affecting the DSIF-RNAPII interaction. Binding of HDAg-S to RNAPII was strongly impaired by a deletion of eight amino acids from its COOH-terminus, whereas the NH₂-terminal segment—including the oligomerization domain, NLS, and a part of the RNA-binding domain—was dispensable (Fig. 3B). Thus, amino acids 130 to 195 of HDAg-S are sufficient for RNAPII binding. The COOH-terminus of HDAg-S is conserved among different genotypes of HDV (16), but to date, no function has been assigned to this region.

To directly measure the effect of HDAg on elongation, we used reactions containing purified RNAPII and deoxycytidine (dC)-tailed templates. In the presence of 4NTPs, transcripts of increasing lengths appeared with time, and DSIF/NELF inhibited this process (Fig. 2C) (4). The addition of HDAGs strongly stimulated RNAPII elongation, irrespective of the presence of DSIF/NELF, whereas the HDAg-S mutant lacking 31 ami-

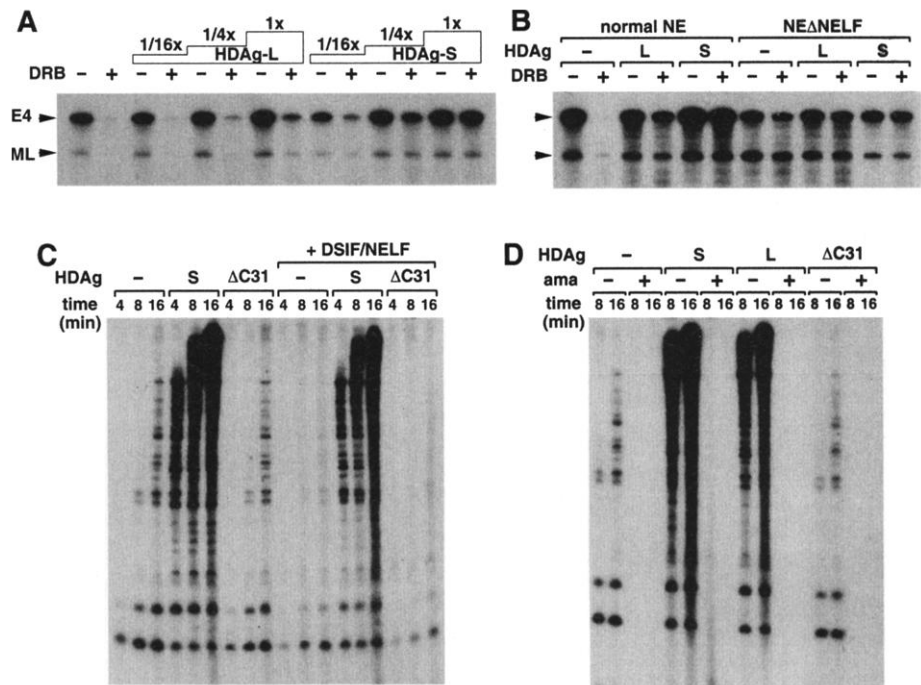
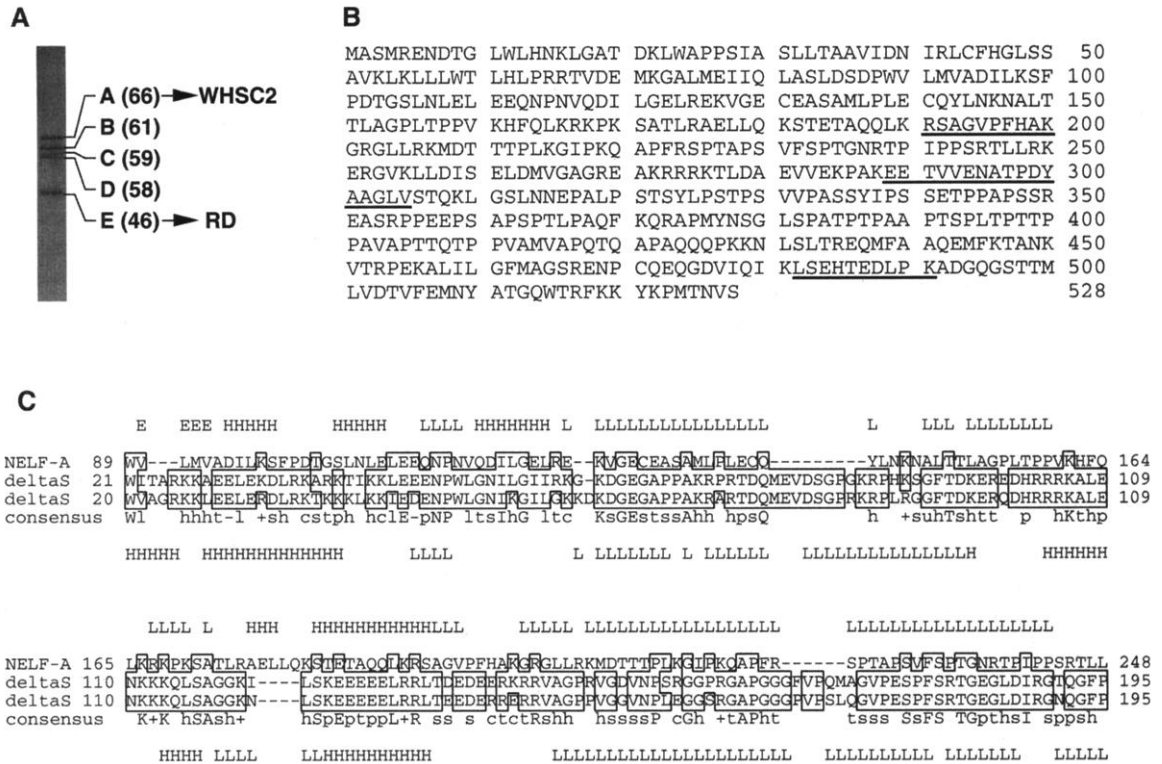


Fig. 2. HDAGs stimulate DNA-templated transcription with crude (A and B) or purified (C and D) transcription systems. (A) Increasing amounts of HDAGs (12, 50, and 200 ng) were added to transcription reactions containing NE, as described (4, 26). DRB (50 μM) was included where indicated. Upper and lower bands represent 380- and 270-nt G-less transcripts from the adenovirus E4 and major-late promoters, respectively. (B) HDAGs (200 ng) were added to reactions containing either untreated or NELF-immunodepleted NE. [(C) and (D)] WT or mutant HDAG (100 ng) was incubated with purified RNAPII and dC-tailed templates with or without DSIF and NELF (4, 27). α-Amanitin (ama) (1.0 μg/ml) was included where indicated.

Fig. 1. NELF-A is encoded by WHSC2. (A) NELF from the final purification step was visualized by silver staining. Molecular sizes (in kD) of the subunits are indicated in parentheses. (B) Amino acid sequence of human NELF-A/WHSC2. The three obtained peptide sequences (underlined) match parts of the predicted human WHSC2 protein (22). (C) Sequence comparison of NELF-A/WHSC2, HDAg-S (genotype IA, P35884), and HDAg-S (genotype IB, 225754). The homology was initially identified through a search against the ProDom database (23) with NELF-A/WHSC2 as a query. Identical residues are boxed. Abbreviations used are c, charged; h, hydrophobic; l, aliphatic; p, polar; s, small; t, turnlike; u, tiny, and +, positive (24). Also shown are the secondary structures as predicted by the program PHD (25). Only positions with the predicted accuracy greater than 82% are indicated (E, sheet; H, helix; L loop). Single-letter abbreviations for the amino acid residues are as follows: A, Ala; C, Cys; D, Asp; E, Glu; F, Phe; G, Gly; H, His; I, Ile; K, Lys; L, Leu; M, Met; N, Asn; P, Pro; Q, Gln; R, Arg; S, Ser; T, Thr; V, Val; W, Trp; and Y, Tyr.



REPORTS

no acids at the COOH-terminus ($\Delta C31$) was inactive (Fig. 2, C and D). These results suggest that the HDAG-RNAPII interaction not only counteracts the repression by DSIF/

NELF but can also stimulate RNAPII elongation in a DSIF/NELF-independent manner. In crude NE (Fig. 2, A and B), the presence of factors that stimulate transcription more effi-

ciently than HDAG might obscure the DSIF/NELF independent effect of HDAG.

To investigate the role for HDAG in HDV RNA replication, we used a previously de-

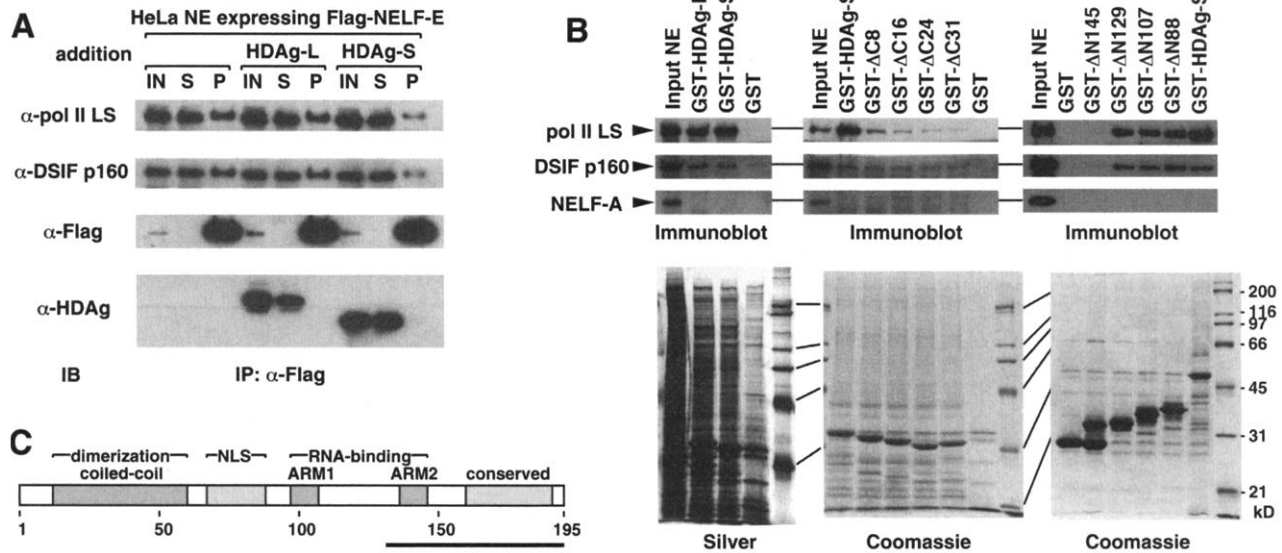
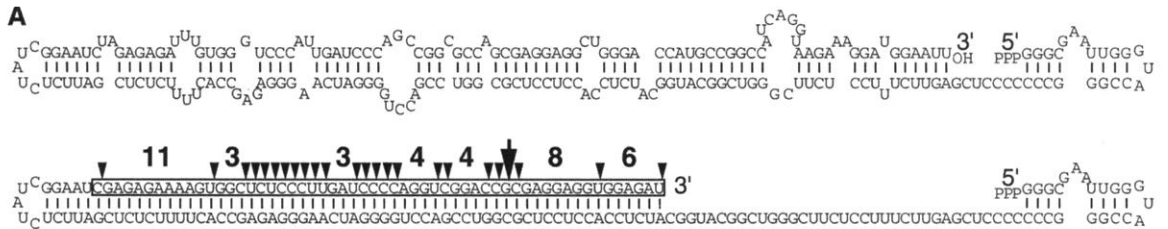


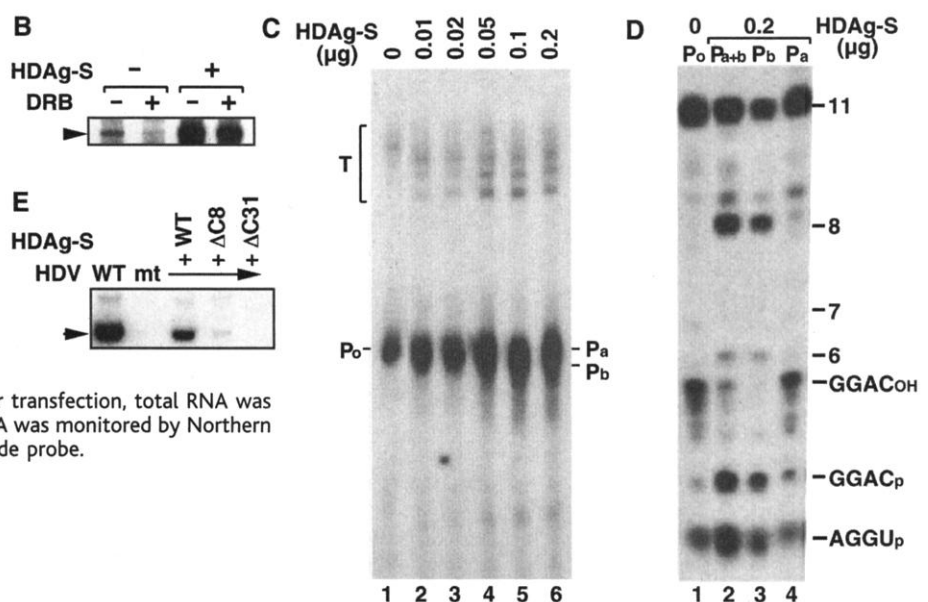
Fig. 3. Direct interaction between HDAGs and RNAPII. (A) HDAG-S inhibits interaction between NELF and DSIF/RNAPII. NE obtained from HeLa cells constitutively expressing Flag-NELF-E was incubated with either HDAG-S or HDAG-L (the amounts correspond to the "1/4 \times " amounts used in Fig. 2A) for 45 min in transcription buffer containing 100 mM KCl and 0.1% Nonidet P-40. The mixture was immunoprecipitated with anti-Flag, and the precipitates (P) were analyzed by immunoblotting with the indicated antibodies (28). Input (IN)

and supernatant (S) lanes represent 2% of the total material. (B) Various GST-HDAG derivatives ($\sim 1.0 \mu\text{g}$) were coupled to glutathione-Sepharose and incubated with NE (100 μl). After extensive washing with the transcription buffer containing 100 mM KCl and 0.1% Nonidet P-40, bound materials were analyzed by immunoblotting and by silver- or Coomassie-staining. (C) Structure of HDAG-S. A solid bar corresponds to the minimal region required for RNAPII-binding. NLS, nuclear localization signal, and ARM, arginine-rich motif.

Fig. 4. HDAG stimulates HDV RNA-templated transcription. (A) Sequences of the template AG103 (top) and the product Pb (bottom). The 3' end of Po and Pa is marked with an arrow. RNase A cleavage sites are indicated by triangles.



The segment transcribed by RNAPII is boxed. (B) HDV RNA template, AG103, and HeLa NE were incubated in the presence of [α - ^{32}P]GTP (17), with (+) or without (-) DRB (50 μM) and HDAG-S (200 ng). (C) The same reaction products were resolved in a 5% polyacrylamide-8 M urea gel. Positions of nonspecifically labeled templates (T) and specific products (Po, Pa, and Pb) are indicated. (D) The reaction products from (C) (lanes 1 and 6) were gel purified, subjected to exhaustive RNase A digestion, and resolved in a 25% polyacrylamide-8 M urea gel. Pa+b is a mixture of Pa and Pb. (E) Plasmids expressing HDV RNA-pSVL(D3) (WT) or pSVL(D2m) (not expressing HDAG)—were introduced into HeLa cells with or without an additional HDAG expression plasmid. Three days after transfection, total RNA was isolated and the level of 1.7-kb genomic HDV RNA was monitored by Northern blotting with an antigenomic-sense oligonucleotide probe.



scribed model system in which RNAPII in HeLa NE transcribes a specific segment of HDV RNA (17). This reaction involves cleavage of the RNA template at a unique site followed by extension of the new 3' end, generating a chimeric template/transcript product (Fig. 4A). Transcription discontinued after copying 41 nt of the template, suggesting that this region of HDV RNA contains a pause signal, and/or that some protein factors required for transcription are limiting in the reaction (17). DRB inhibited this reaction, indicating that DSIF/NELF participates in the RNA-templated transcription (Fig. 4B). The addition of HDag-S reversed the DRB-mediated inhibition and strongly stimulated basal transcription (Fig. 4B), suggesting that HDag-S affects the RNA-templated transcription through both DSIF/NELF-dependent and -independent mechanisms, as observed with purified RNAPII (Fig. 2, C and D).

Upon better resolution of products of the HDag-S-supplemented reactions, two distinct RNAs were detected (Fig. 4C). Analysis of ribonuclease (RNase) A digests of these RNAs demonstrated that, whereas the slower migrating product (Pa) is identical to Po formed in the absence of HDag, the faster migrating product (Pb) is a previously unknown species, extended at its 3' end by at least 15 nt (Fig. 4, A and D). The unusually fast mobility of Pb probably results from the presence of an extended double-stranded segment in its structure. These results suggest that HDag stimulates HDV RNA replication by suppressing RNAPII pausing at +41. Unexpectedly, this position corresponds to the primary site of DSIF/NELF repression during RNAPII elongation on DNA (4).

To elucidate the physiological relevance of these findings, we compared the ability of wild-type (WT) and mutant HDags to support in trans replication of the HDag-defective HDV mutant. WT HDag-S, but not ΔC8 or ΔC31, supported replication of

the defective virus (Fig. 4E). Therefore, the same region of HDag is required for efficient RNAPII elongation in vitro and HDV RNA replication in vivo.

These results establish that HDag directly binds RNAPII and stimulates transcription by two different mechanisms: It reverses the negative effect of DSIF/NELF by displacing NELF from RNAPII and directly stimulates transcription elongation. This is, to our knowledge, the first example of a viral protein that regulates elongation through direct binding to RNAPII. Nonetheless, similarity between HDag and human immunodeficiency virus (HIV) Tat is intriguing. During HIV transcription, Tat stimulates RNAPII elongation by recruiting P-TEFb and reversing the negative effect of DSIF/NELF immediately downstream of the promoter (18).

HDV RNA resembles the genomes of plant viroids, although viroid RNAs are much smaller (<400 nt) and contain no open reading frames. This has led to a hypothesis that HDV may have evolved from a primitive viroidlike RNA through capture of a cellular transcript (19). Previously, a putative cellular homolog of HDag was identified (20). This protein, termed DIPa, is 24% identical to HDag but shows no apparent sequence similarity with NELF-A (15). The low levels of sequence similarity make it difficult to define evolutionary relationships of the three proteins. Regardless of its evolutionary origin, the HDag-RNAPII interaction is critical for HDV replication and could be used as a therapeutic target against this pathogenic virus.

References and Notes

1. J. W. Conaway, A. Shilatifard, A. Dvir, R. C. Conaway, *Trends Biochem. Sci.* **25**, 375 (2000).
2. T. Wada *et al.*, *Genes Dev.* **12**, 343 (1998).
3. T. Wada, T. Takagi, Y. Yamaguchi, D. Watanabe, H. Handa, *EMBO J.* **17**, 7395 (1998).
4. Y. Yamaguchi *et al.*, *Cell* **97**, 41 (1999).

5. J. B. Kim, P. A. Sharp, *J. Biol. Chem.* **276**, 12317 (2001).
6. Y. Yamaguchi, T. Wada, H. Handa, *Genes Cells* **3**, 9 (1998).
7. G. Hartzog, T. Wada, H. Handa, F. Winston, *Genes Dev.* **12**, 357 (1998).
8. T. Wright, J. L. Costa, C. Naranjo, P. Francis-West, M. R. Altherr, *Genomics* **59**, 203 (1999).
9. M. M. Lai, *Annu. Rev. Biochem.* **64**, 259 (1995).
10. M. Y. Kuo, M. Chao, J. Taylor, *J. Virol.* **63**, 1945 (1989).
11. L. E. Modahl, M. M. Lai, *J. Virol.* **74**, 7375 (2000).
12. F.-L. Chang, P.-J. Chen, S.-J. Tu, C.-J. Wang, D.-S. Chen, *Proc. Natl. Acad. Sci. U.S.A.* **88**, 8490 (1991).
13. K. Lo, G. T. Sheu, M. M. Lai, *Virology* **247**, 178 (1998).
14. Y. Wei, D. Ganem, *J. Virol.* **72**, 2089 (1998).
15. Y. Yamaguchi *et al.*, data not shown.
16. J. L. Casey, T. L. Brown, E. J. Colan, F. S. Wignall, J. L. Gerin, *Proc. Natl. Acad. Sci. U.S.A.* **90**, 9016 (1993).
17. J. Filipovska, M. M. Konarska, *RNA* **6**, 41 (2000).
18. E. Garber, K. A. Jones, *Curr. Opin. Immunol.* **11**, 460 (1999).
19. H. D. Robertson, *Science* **274**, 66 (1996).
20. R. Brazas, D. Ganem, *Science* **274**, 90 (1996).
21. V. V. Bichko, J. M. Taylor, *J. Virol.* **70**, 8064 (1996).
22. The identity of NELF-A was confirmed with the use of an antibody against recombinant WHSC2, which recognized the 66-kD polypeptide NELF-A (Fig. 3B).
23. F. Corpet, J. Gouzy, D. Kahn, *Nucleic Acids Res.* **26**, 323 (1998).
24. W. R. Taylor, *J. Theor. Biol.* **119**, 205 (1986).
25. B. Rost, C. Sander, *J. Mol. Biol.* **232**, 584 (1993).
26. HDag cDNAs (gifts from M. Lai) were cloned into pET-14b (Novagen, Milwaukee, WI), and recombinant proteins were expressed in BL21-CodonPlus (DE3)-RP (Stratagene). His-tagged HDag proteins were purified from gel slices and renatured by dialysis. HDags used in Fig. 4 (C and D) were provided by J. Doudna. GST-HDag proteins were made from pGEX-6P1 (Amersham Pharmacia) derivatives.
27. DSIF was an equimolar mixture of recombinant hSpt5 and hSpt4 made in *Escherichia coli* (2).
28. Anti-RNAPII CTD (8WG16) and anti-Flag (M2) were purchased from Babco and Sigma. Anti-DSIF p160 (2) and anti-HDag (27) were as described.
29. We thank M. Lai, J. Taylor, and J. Doudna for providing reagents, and K. Chayama, M. Altherr, and D. Colgan for helpful discussions and comments on the manuscript. We also thank M. Usui for secretarial support and J. Kato for technical assistance. Supported by a Grant-in-Aid for Scientific Research on Priority Areas from the Ministry of Education, Sciences, Sports and Culture of Japan and a grant from the New Energy and Industrial Technology Development Organization to H.H.

30 November 2000; accepted 14 May 2001
 Published online 31 May 2001;
 10.1126/science.1057925
 Include this information when citing this paper.

Enhance your AAAS membership with the Science Online advantage.

- **Full text Science**—research papers and news articles with hyperlinks from citations to related abstracts in other journals before you receive *Science* in the mail.
- **ScienceNOW**—succinct, daily briefings, of the hottest scientific, medical, and technological news.
- **Science's Next Wave**—career advice, topical forums, discussion groups, and expanded news written by today's brightest young scientists across the world.

- **Research Alerts**—sends you an e-mail alert every time a *Science* research report comes out in the discipline, or by a specific author, citation, or keyword of your choice.
- **Science's Professional Network**—lists hundreds of job openings and funding sources worldwide that are quickly and easily searchable by discipline, position, organization, and region.
- **Electronic Marketplace**—provides new product information from the world's leading science manufacturers and suppliers, all at a click of your mouse.

All the information you need....in one convenient location.

Visit Science Online at <http://www.scienceonline.org>, call 202-326-6417, or e-mail membership2@aaas.org for more information.

AAAS is also proud to announce site-wide institutional subscriptions to Science Online. Contact your subscription agent or AAAS for details.

Science ONLINE

 AMERICAN ASSOCIATION FOR THE ADVANCEMENT OF SCIENCE